

Balancing Domain Gap for Object Instance Detection*

Woo-han Yun, Jaeyeon Lee, Jaehong Kim, and Junmo Kim

Abstract— Object instance detection in cluttered indoor environment is a core functionality for service robots. We can readily build a detection system by following recent successful strategy of deep convolutional neural networks, if we have a large annotated dataset. However, it is hard to prepare such a huge dataset in instance detection problem where only small number of samples are available. This is one of main impediment to deploying an object detection system. To overcome this obstacle, many approaches to generate synthetic dataset have been proposed. These approaches confront the domain gap or reality gap problem stems from discrepancy between source domain (synthetic training dataset) and target domain (real test dataset). In this paper, we propose a simple approach to generate a synthetic dataset with minimum human effort. Especially, we identify that domain gaps of foreground and background are unbalanced and propose methods to balance these gaps. In the experiment, we verify that our methods help domain gaps to balance and improve the accuracy of object instance detection in cluttered indoor environment.

I. INTRODUCTION

The development of deep learning brings tremendous progress to object detection system and leads to the system being deployed in the real-world tasks such as autonomous driving, visual surveillance, medical imaging and robotics. Imagine you build an object detection function for a robot to assist you cooking or woodworking. This robot has to recognize not only object categories such as bottle, dish, cup, and hammer, but also distinguish different object instances in same category such as your bottle and my bottle in a single category. This type of object detection is called object instance detection.

With the help of recent successes of deep convolutional neural networks in object detection tasks [1]–[3], object instance detection systems may be easily built by following ordinary training steps, collecting dataset and learning the system with powerful parallel processing hardware. But in case of instance detection problem, it is difficult to collect large amount of training dataset of the new object instance, especially in robotic service scenarios. Furthermore, the training dataset should include a range of images captured under various circumstances such as viewpoints, illuminations, and backgrounds with their annotated bounding boxes.

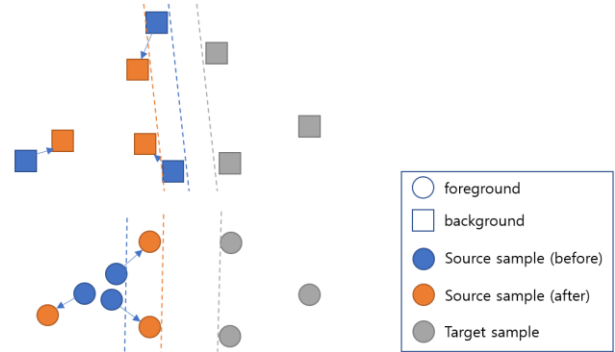


Figure 1. Data points of foreground (circle) and background (square) in source (blue and orange) and target domain (gray).

Recent successful approach to overcome this barrier is to use rendered scenes and objects using 3D models [4]–[6][7], [8][9]–[14]. If we are able to use 3D models, we can generate diverse images for training dataset. However, in a household environment, making accurate 3D model is not a simple task. Furthermore, making realistic scenes and objects requires a lot of effort and professional skills. Moreover, models trained on such a synthetic dataset suffered from reality gap problem which several approaches have tried to overcome [5], [6], [8]. Another approach is to make synthetic training dataset directly from real images [15], [16]. The object area is segmented and pasted on the randomly selected real background images for making training dataset. This approach requires mask information instead of 3D models, which can be generated automatically [15] or manually [16].

Our work is based the second approach, making training dataset from real object and background images. Similar with other computer vision problems, this approach also assumes that training domain (or source domain) is same with the test domain (or target domain). This means the training images and test images are sampled from same distribution. However, this assumption is broken because it is hard to capture all possible situations of testing environment at a training stage. This situation is displayed in Figure 1. If we consider rapid deployment at working environment, we may collect object instance images under limited environment (e.g. capturing images on the table in the monotone lighting environment). This data could not have diversity and be gathered (blue circle). We also prepare the background scenes beforehand (e.g. using public dataset). This background images are collected in diverse situations and the data is scattered (blue square). These object images and background scenes are not collected in a testing environment (target domain). This means the distribution of training samples (blue square and circle) and that of test samples (gray square and circle) are not identical. Many models trained on synthetic datasets suffer from performance degradation by this domain gap or reality gap [5] (gap between blue dotted lines and gray dotted lines).

* This work was supported by the ICT R&D program of MSIP/IITP. [2017-0-00162, Development of Human-care Robot Technology for Aging Society].

W. Yun is with Robotics Program, KAIST and Intelligent Robotics Research Division, ETRI, Republic of Korea (yochin@kaist.ac.kr, yochin@etri.re.kr).

J. Lee and J. Kim are with Intelligent Robotics Research Division, ETRI, Republic of Korea ({leejy, jhkim504}@etri.re.kr).

J. Kim is with School of Electrical Engineering, KAIST, Republic of Korea (junmo@ee.kaist.ac.kr).

In this work, we notice that the domain gap of foreground and background is different and introduce to reduce the gap of domain gaps (blue circle and square to orange ones).

We conduct the experiment under the assumption that we can access only a few target images. We measure the domain gap between source domain (training dataset) and target domain (test dataset). Especially, we compare two domain gaps of foreground and background and identify that the domain gap is unbalanced. Next, the step-by-step methods are introduced to mitigate this gap of domain gaps. Finally, we validate the proposed methods are helpful to balance domain gaps and improve the object detection performance.

Our work contains two key contributions: 1) We newly define the domain gap problem of object instance detection using a synthetic dataset as the unbalanced gap of domain gaps of foreground and background images. 2) Our work proposes methods for foreground and background images to alleviate this unbalanced gap of domain gaps without information of target domain and shows higher detection accuracy with fewer foreground images.

II. RELATED WORK

Object instance detection has been studied in computer vision and robotics. In the early studies, many handcrafted features such as SIFT [17] and SURF [18] for texture-rich objects and shape-based methods [19][20] for texture-poor objects are used for object instance detection.

Recent detection methods [1][3][2][13] are based on multilayer convolutional neural networks (CNNs). Because feature extraction layers of the network have great many trainable parameters, these layers are transferred from other networks [21]–[23][24] trained on massive training dataset such as ImageNet [25]. Based on these feature extraction layers, specialized architectures for fast object detection are proposed such as Faster-RCNN [1], SSD [2] and Yolo [3].

These object detection algorithms commonly require a large labeled training dataset. The dataset should have not only a large number of images, but also include various variations. This requirement is hard to satisfy when we apply this system into home or others.

To overcome this barrier, one way is to use rendered image dataset. In this approach, the synthetic image dataset is generated by rendering whole scenes [5], [9]–[11] or composing rendered objects on the real image background [4], [12]–[14]. These rendered datasets have various object images by rendering 3D models from different viewpoints, but struggles with the performance degradation by reality gap between rendered training dataset and real test dataset. Recent works [4][6][5][7] introduce this domain gap could be reduced by domain randomization technique.

Alternative approaches [15], [16] use a synthetic dataset generated by placing real segmented object images on the real background images. This approach needs segmentation information such as a mask instead of 3D models. Previous works get this information automatically [15] or manually [16] and place the segmented object on the real backgrounds in randomly [15] or according to its scene context [16]. They focus on where and how placing the object instances on the background scenes.

These approaches using synthetic training dataset suffer from domain gap or domain shift problem because their training domain does not completely coincide with test domain. To cope with this problem, domain adaptation is widely studied in computer vision and machine learning [26][27][28][29]–[31]. Recent works introduce a domain adaptation methods on the deep learning framework [32]–[37][38]. These many previous works have focused on object classification problem. Although less attention was paid to domain adaptation for object detection task, some works [39]–[42] have been researched. They presented adaptive structural SVM for DPM-based object detector [39], adaptive decorrelation approach based on the data statistics [40], subspace alignment on feature representations [41], and reduction of domain gap by adversarial training manner [42]. There are researches [43][44][45][46] to use generative adversarial networks for domain adaptation in pixel-levels. These works commonly require information about target domain through unlabeled or a low number of target-domain samples.

III. DOMAIN GAP

Many computer vision problems assume that training and test data are sampled from an identical distribution or in same domain. Therefore, the trained system works well when the environment of training and testing is similar or testing environment is a subset of training environment. However, this assumption is not applicable to many systems. In our work, the synthetic training dataset is generated from two image sources, object instance images and background images. Object instance images are captured in a limited environment (e.g. limited lighting condition) and background images are collected in advance from different places. This situation entails domain gap between training data (source domain) and test data (target domain).

Compared with ordinary domain gap problems, our work utilizing a synthetic dataset generated from two sources (real object and background images) has an additional point, that is the amount of domain gaps of foreground objects and background scenes is quite different. This could be considered as unbalanced domain gap problem. To compare the domain gaps of foreground (object instances) and background (background scenes), we utilize H -divergence [42][47] that is designed to measure the divergence between two sets of samples from different domains or distributions. Let S and T be a set of source and target domain, respectively. x is a feature vector of a sample from S or T . h is one of domain classifiers in H to classify S and T given x . H is a set of possible domain classifiers. H -divergence is defined as follows:

$$d_H(S, T) = 2 \left(1 - \min_{h \in H} (err_S(h(x)) + err_T(h(x))) \right) \quad (1)$$

where err_S and err_T is the prediction error of domain classifier h given a sample x from source and target domain, respectively. H -divergence implies that the domain distance $d_H(S, T)$ depends on how well samples of each domain is separable. If the samples are well separable, it means their distance is quite far and the prediction error will be low. Therefore, the H -divergence is inverse proportional to the prediction errors.

To measure H -divergence in our problem, we prepare the dataset and classifier set H . We first made a dataset that has

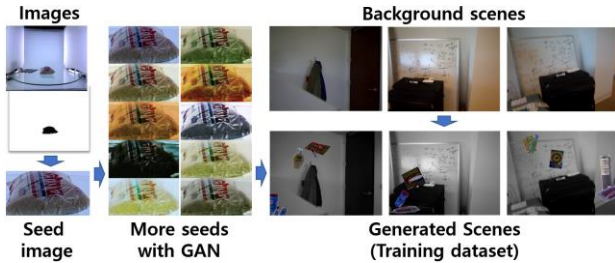


Figure 2. Overview of our approach to generate dataset. Starting from a set of object images and masks, diverse seed images are generated using GAN and pasted on the image processed background scene.

10,000 patches with 32x32 pixels of foreground and background. Foreground patches are randomly cropped in a bounding box of object instances. Background patches are selected in background area to be $\text{IoU} < 0.1$ with the bounding boxes of object instances. The considered classifier is a simple convolutional neural networks with an architecture of conv(k5-f6)-maxp(k2)-conv(k5-f16)-maxp(k2)-fc1(f120)-fc2(f84)-fc3(f2) where k5 means a kernel with 5x5 and f6 means a filter size with 6. ReLU activation function is applied after every conv and fc layers except for the last layer. We use a simple architecture because the patch size was relatively small to use other heavy architectures such as VGG [21] or ResNet [23]. We split the dataset into training, validation, and test with 70%, 10%, and 20%, respectively. Each set do not share same backgrounds or scenes. We select the best classifier having the best validation accuracy. H -divergence we measured is in Table 1.

TABLE I. H -DIVERGENCE OF FOREGROUND AND BACKGROUND PATCHES BETWEEN SOURCE DOMAIN AND TARGET DOMAIN. H -DIVERGENCE OF FOREGROUND IS LARGER THAN THAT OF BACKGROUND.

| | foreground | background |
|-----------------|------------|------------|
| H -divergence | 1.616 | 1.016 |

From Table 1, we identify that the domain gap of foreground and background is unbalanced, 1.616 and 1.016. This means foreground patches are easily distinguishable between training set (source domain) and test set (target domain), but background is relatively hard to distinguish. If we have an information of target domain in advance, we could utilize this information to reduce domain gap by reducing H -divergence [42]. In this work, we propose this unbalanced domain gap to be balanced without information of target domain.

IV. BALANCING DOMAIN GAP

The overall process mainly follows previous research [15], but some steps are modified to balance the domain gaps of foreground and background images. Our method consists of collecting images of object instances and background scenes, processing collected images, and pasting object areas on background scenes. The overview of our approach is in Figure 2.

1. Collect object images: Take photos of object instances from each surface and corners to cover diverse view-points. These images are used as seed images to make synthetic training dataset.

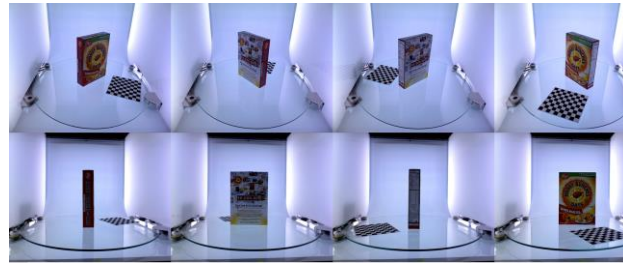


Figure 3. Eight seed images of *honey bunches* class. Top four images are used for testing four seed images. The first and third at the first row are used for two seed images.

2. Collect background scene images: These images will be used as a background. This step could be replaced by preparing public dataset.
3. Predict foreground mask: This step is to make masks of object instance images. These masks are used to segment the object instances from the images.
4. Deteriorate background images: To expand the domain gap of background images, we deteriorate its image quality with image processing technique.
5. Enrich foreground images: To reduce the domain gap of foreground images, we generate more diverse foreground images to be used as seed images.
6. Paste object instances on background scenes: Finally, paste segmented object instances on a randomly chosen background images. To reduce local artifacts at the object boundaries, we adopt the method in [15]. We also apply data augmentation to simulate variations such as translation, rotation, and scales of object instances.

We provide more details of our approach such as what database and design we used and why we choose those.

A. Collect object images

We first collect the real images of object instances. Instead of collecting real object images, we used object instance in Big Berkeley Instance Recognition Dataset (BigBIRD) [48]. In the dataset, 125 object instances have 600 images taken from different view-points of five elevations and 360 angles. In the previous research, all images (600 in [15]) or some parts of images (360 in [16]) were used as seed images to make synthetic training dataset. To reduce human efforts to capture object images and make masks (if that is not automatic process), we also consider to reduce the number of seed images of objects. We select images to be seen as many faces as possible in one image. We considered two, four, and eight number of images as a few-shot seed images. The seed images we used are in Figure 3.

B. Collect background scene images

Object images of the BigBIRD Dataset are captured under limited environment such as modest backgrounds and monotonous lighting conditions. To reflect more realistic and diverse backgrounds, we place the extracted objects on real background images randomly sampled from 1548 images in the background subset of UW Scenes dataset [49].



Figure 4. The generated seed images using MUNIT [46]. The first column is input images from BigBIRD Dataset. The second column is generated image without style codes. The other columns are with randomly sampled styles. Images in same column generated from same style code.

C. Predict foreground mask

In order to extract the object instance area in a seed image, we need to determine which pixels belongs to the foreground (object instance area) against the background area. This step could be done manually with GrabCut [50] or automatically with semantic segmentation algorithms [51], [52]. If we have only small number of seed images, manual segmentation is not a big burdensome. In our experiment, the test using 360 and 600 seed images uses masks generated manually in the previous experiment [16] and provided in BigBIRD Datasets [48], respectively. Segmentation masks in BigBIRD Dataset is automatically generated from point clouds by removing all points below turntable plane [48]. Masks of two, four, and eight seed images are generated by manually using GrabCut algorithm [50]. All masks are refined with a hole-filling algorithm to remove inner holes in masks.

D. Deteriorate background images

To expand the domain gap of background between source domain (training dataset) and target domain (test dataset), we deteriorate background images with image processing such as gaussian blurring (to attenuate its high frequency information), graying, and quantizing color to 8 bits (to lose its color information). We expect that all these processes cause background images to be unrealistic and the domain gap of background to be enlarged. In the experiment, we validate that this process expands its domain gap.

E. Enrich foreground images

To reduce the domain gap of foreground (object instance), we generate diverse seed images with the generative adversarial network (GAN). As a GAN model, we use a Multimodal Unsupervised Image-to-image Translation (MUNIT) model [46]. In this model, the image is decomposed

into a content code that is domain-invariant and a style code that is domain-specific. The image could have other styles by combining the content code with other random style codes. This model could be trained without pair-wised dataset in source and target domain. For training, we used the images in BigBIRD Dataset and Active Vision Dataset (AVDataset) [53] as source and target domain, respectively. The used object instances are not in GMU Kitchen, but in AVDataset because GMU Kitchen dataset is used for evaluation. The result images are in Figure 4. All results in same column are generated with same style code. Images in the first and second column are input images and result images generated without style code (by giving zero code), respectively. We identify that the learned styles are mainly lighting effects such as spot lights and color tone of lights. With MUNIT model, we can insert various style effects to the object instance image.

F. Paste foregrounds on backgrounds

The final step is to paste the segmented and processed object seed images on the randomly chosen background scene. We follow the previous work research [15] where the object instance is randomly scaled, rotated, and positioned on the background images with blending methods for reducing the artifacts of the boundary. Instead of the random position of the object instance in the original work, we place the object instance to be more overlapped with other objects.

V. EXPERIMENTS

In the experiment section, we test the object detection performance along with the number of seed images. Then we compare the domain gap of foreground and background before and after the propose methods. Finally, we apply our method on public benchmark datasets. We first describe common experimental setups.

Dataset: We use 11 object instances overlapped on both BigBIRD Dataset [48] and GMU Kitchen Dataset [54] for reporting object instance detection performance. The images in BigBIRD Dataset are used as seed images and those in GMU Kitchen Dataset are used for evaluation. 1548 background images in UW Scenes Dataset [49] are used for background dataset. 26 object instances in AVDataset [53] are used to train a MUNIT model in Section 4.E. We only use object instances those are not included in GMU Kitchen Dataset for training the MUNIT model.

Data augmentation: We utilize the source code [55] to make the synthetic dataset. The default options in the previous work [15] are used as default setting values. Those are 2D rotation (angles uniformly sampled from -30 to 30 degrees), scales (from 0.25 to 0.6), occlusion (allowing maximum IOU of 0.75 between objects), and truncation (allowing at least 25 percentage of the objects in the image). Two to four objects sampled from BigBIRD Dataset not included in GMU Kitchen Dataset are used as distractor objects. One to four object instances are sampled from seed images for each synthetic image. We generate the final synthetic training dataset with approximately 6000 images with 640x480 pixels. We find that placing objects in random positions in [15] rarely causes occlusion. To make more occlusions, we select the position of the object instances to be near the previous position of the other objects with a 50 percent chance. We name this version as *occV2* against the original one.

Model and learning: We use a PyTorch version [56] of Faster R-CNN architecture [1] based on VGG-16 [21]. The network is initialized with the weights pretrained on the MSCOCO [57], then finetuned on each synthetic dataset. The network was trained for 4 epochs using SGD+momentum optimizer with learning rate 0.001, momentum 0.9. The learning rate was reduced by a factor of 10 after 2 epochs. For consistent evaluation, we fixed all hyperparameters and random seed across experiments. For training MUNIT model, we use a PyTorch code [58] with the synthia2cityscape settings. We add Laplacian loss [59][60] to preserve a detail-enhanced images. The images resized to 384x384 pixels are used for both source and target domains. The model is trained for 300,000 iterations with a batch size 1.

Evaluation: Accuracy is reported in mean Average Precision (mAP) at IOU of 0.5. We report mAP calculated using PASCAL VOC matlab code [61]. Boxes at least 50 x 30 pixels are used as an evaluation to follow previous works [15][16].

A. Limited seed images to generate training dataset

In the previous research [15], [16], they use as much as seed images to generate training dataset, 600 viewpoint images in [15] and 360 viewpoint images in [16] for each object instance. If we can acquire similar accuracy with fewer seed images, we have several advantages such as alleviating human efforts to capture images, getting more complete masks by manual segmentation, and being applicable the system to the limited capture environment.

To show that the performance degradation is not significant with the fewer seed images, we conduct the experiment with a range of seed images. The considered number of seed images were 2, 4, 8, 360, and 600 for each object instance. We also report the result from [15], [16] and the result trained with real images in GMU Kitchen dataset. We note that [16] uses 360 seed images and around 7000 background images from NYUD v2 Dataset [62]. They utilize global structure information (e.g. objects on flat surfaces) to paste images. The work [15] pastes object images randomly on the background images from UW Scenes Dataset [49].

TABLE II. EVALUATION ON TRAINING DATASETS BY VARIING THE AMOUNT OF SEED IMAGES FROM 600 TO 2. REAL MEANS THE RESULT TRAINED ON REAL IMAGES. SYN AND NUMBER MEANS THE USED NUMBER OF SEED IMAGES FOR THYNTHETIC DATASET

| # of seed images | mAP |
|------------------|------|
| Real [15] | 86.3 |
| Syn600 [15] | 76.2 |
| Real [16] | 82.5 |
| Syn360 [16] | 51.7 |
| Real | 86.2 |
| Syn600 | 71.6 |
| Syn360 | 72.8 |
| Syn8 | 67.2 |
| Syn4 | 60.2 |
| Syn2 | 54.9 |

Table 2 shows the evaluation result on training datasets by varying the amount of seed images from 600 to 2. Even though

the model is trained on same real images (rows 1, 3, 5), they show different accuracy. This also happens in synthetic dataset with 600 (rows 2 vs 6) and 360 (rows 4 vs 7) seed images. We guess this performance difference stems from difference of the detailed options of training models, used background and masks. Comparing with fewer seed images with others (rows 6 to 10), the accuracy was dropped from 71.6% and 72.8% to 67.2% by 4.4% and 5.6%, respectively. We decide that the degradation is not severe when we consider the fewer seed images. Therefore, in the following experiment, we use eight seed images.

B. Deteriorating background images

To see the effect of degradation on background, we apply three image processing techniques, gaussian blurring, gray conversion, and 8-bit color quantization, to background images. To inspect the deterioration effect of a variety of background images, we test more experiments with other public datasets, COCO [57] and NYUDv2 Dataset [62]. We selected 1,500 images from the original dataset and used them randomly as background images in all background cases. Table 3 shows that evaluation results of three image processing on three background scenes. We observe that detection accuracy depends on the types of original background. When the background images are properly similar with the target domain (UW Scenes and NYUDv2 both include a variety of indoor scenes), then detection accuracy is high (col 1, 3 in Table 3). But the background includes too various kinds of scenes (COCO has a range of images such as foods, vehicles, animals, indoor and outdoor scenes, etc.), the accuracy was low (col 2 in Table 3). We guess that this diversity of background images hinders the proper gap between source and target domains in comparison with that of foreground images. Regardless of background types, all degradation methods contribute to improve its accuracy of object detection on all background scenes. Especially removing color information by converting to gray scale increases its accuracy by 8.1%, 32.3%, and 5% on each background dataset, respectively. This is coincided with the result in the previous work [13].

TABLE III. EVALUATION ON THREE IMAGE PROCESSING AND VARIOUS BACKGROUND SCENES.

| Degradation method | mAP | | |
|--------------------|-----------|------|--------|
| | UW Scenes | COCO | NYUDv2 |
| w/o processing | 67.2 | 42.4 | 71.2 |
| Gaussian blur | 72.7 | 74.3 | 73.7 |
| Gray | 75.3 | 74.7 | 76.2 |
| 8-bit quantization | 72.8 | 65.3 | 73.0 |

C. Enriching foreground images

Based on the result (Gray, row 1 in Table 4) in Section 5.B, we evaluate the methods for enriching foreground images in terms of object detection performance. Those are generating more occlusion (occV2) and using more seed images generated by GAN (GAN). In Table 4, we identify that generating more occlusion situation (following previous positions with 50%) leads to higher accuracy by about 1% (row 1 vs 2). But this does not mean that higher occlusion lead to higher accuracy because we observe that the performance is decreased when we generate much more occlusions

(following previous positions with 100%). When we train the model on the seed images that is only generated GAN, the performance degraded by about 6% (row 2 vs 3). With the synthetic images generated from both original seed images and GAN seed images with an equal ratio, we get improved accuracy by 1.7% (row 2 vs 4). This is a higher accuracy than results using more seed images (rows 2, 4, 6, and 7 in Table 2).

TABLE IV. EVALUATION ON ENRICHING FOREGROUND IMAGES.

| Enriching method | mAP |
|--------------------|------|
| Gray | 75.3 |
| Gray-occV2 | 76.4 |
| Gray-occV2-GAN | 70.5 |
| Gray-occV2-HalfGAN | 78.1 |

D. Domain gaps

To identify the change of domain gaps before and after our methods, we measure the domain gap using H -divergence in Section 3 and plot the data points with t-SNE [63]. To plot the distribution of data, we use feature vectors at fc2 layers. In Table 5, we observe that the domain gap of foreground is reduced from 1.6 to 1.3 and the gap of background is increased from 1.0 to 1.5. As a result, the gap of domain gaps of foreground and background is reduced from 0.6 to 0.12. In Figure 5, we identify the shift of domain gap. The data points of foreground before and after our methods is in (a) and (c) and the those of background in (b) and (d). From (a) to (c), we can see the data points become more overlapped. On the other hand, the data of background becomes more separated from (b) to (d).

TABLE V. DOMAIN GAP USING H -DIVERGENCE OF FOREGROUND AND BACKGROUND PATCHES WITH AND WITHOUT OUR METHODS. WITH OUR METHODS, THIS GAP BECAME BALANCED AND ITS GAP IS REDUCED.

| H -divergence | foreground | background | Gap |
|-----------------|------------|------------|------|
| Before | 1.616 | 1.016 | 0.60 |
| After | 1.336 | 1.456 | 0.12 |

We expect the process for foreground images generates diverse foreground images in the synthetic dataset. This expands its boundary of foregrounds of source domain and reduced its gap with target domain. Contrary, the process for background images such as graying and blurring shrinks the data distribution (imagine if we blur images with an infinite kernel size, then we get some similar images with one values). This pulls its boundary of background in source domain and expands its gap with target domain.

E. Evaluating on the Active Vision Dataset

To evaluate generalization capability of our methods, we present the experimental result on a cross-domain setting. We train the detection system on our final synthetic dataset (Gray-occV2-HalfGAN in Table 4) and all images of GMU Kitchen dataset and evaluate on the Active Vision Dataset (AVDataset) [53]. The AVDataset includes color and depth images of 33 object instances. The dataset firstly has 17,556 images in 9 scenes and later released 18,540 images of 10 scenes more. In our test, we only evaluate on the first released dataset to compare previous research [15]. We report the result

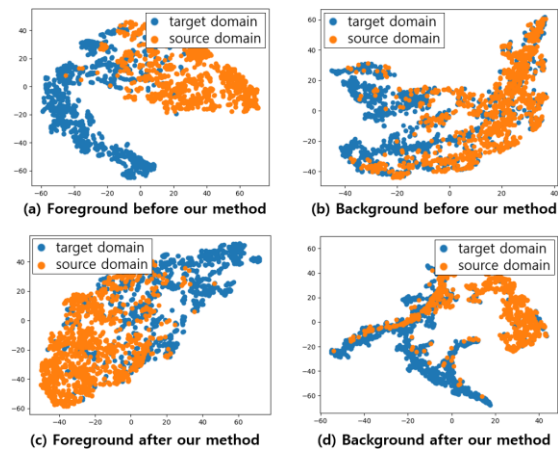


Figure 5. t-SNE visualization of feature vectors at fc2 layers. (a) and (b) is an original data of foreground and background. (c) and (d) is the data after our algorithm.

of six object instances overlapped on GMU Kitchen and AVDataset. We also present the accuracy by varying the number of real images. For this test, we do not train more on AVDataset. In Table 6, the result with models trained on the proposed synthetic dataset generated with only eight seed images is similar with the result with 600 seed images (row 1 vs 4). Moreover, our results with real 100% and 10% is superior than results with syn600 (row 2, 3 vs 5, 6). The result with just 1% real images and our synthetic dataset is higher than that with 10% real images and 600 seed images (row 3 vs 7). This means we can obtain the higher detection performance with only small portion of real images and fewer seed images if we apply our methods.

TABLE VI. EVALUATION ON THE AVDATASET

| Dataset | mAP | coca cola | honey bunches | hunt's sauce | mahatma rice | Nature red bull v2 |
|---------------------|------|-----------|---------------|--------------|--------------|--------------------|
| Syn600 [15] | 36.5 | 63.0 | 29.3 | 34.2 | 20.5 | 49.0 |
| Real+Syn600 [15] | 51.1 | 69.9 | 44.2 | 51.0 | 41.8 | 48.7 |
| 10% Real+Syn600[15] | 43.2 | 66.1 | 36.5 | 44.0 | 26.4 | 48.9 |
| Prop8 | 35.8 | 55.3 | 20.2 | 43.5 | 24.2 | 30.4 |
| Real+ Prop8 | 55.4 | 71.8 | 44.9 | 60.3 | 41.7 | 52.8 |
| 10% Real+ Prop8 | 53.3 | 68.8 | 42.8 | 61.7 | 41.3 | 50.1 |
| 1% Real+ Prop8 | 49.2 | 62.4 | 37.4 | 55.6 | 43.2 | 45.5 |

VI. CONCLUSION

In this work, we presented methods to synthesize training images with seed images. We identified that the domain gap is unbalanced when we paste the seed images on the background scenes to generate a synthetic dataset. To balance the domain gap, we introduced methods for foreground and background images. We plotted the data points before and after our method and observed that the methods are effective to reduce its gap. With the experiments on GMU Kitchen dataset and AVDataset, we verified that our methods are helpful to improve its accuracy and comparable with the method using large number of seed images. Our method can be useful for situations where users train robots with just a few images captured in a restricted environment by improving its detection accuracy.

REFERENCES

- [1] S. Ren, K. He, R. Girshick, and J. Sun, "Faster R-CNN: Towards Real-Time Object Detection with Region Proposal Networks," *IEEE Trans. Pattern Anal. Mach. Intell.*, vol. 39, no. 6, pp. 1137–1149, 2017.
- [2] W. Liu *et al.*, "SSD: Single Shot MultiBox Detector," in *European Conference on Computer Vision*, 2015, vol. 9905 LNCS, pp. 21–37.
- [3] J. Redmon and A. Farhadi, "YOLO9000: Better, Faster, Stronger," in *IEEE Conference on Computer Vision and Pattern Recognition*, 2017.
- [4] Y. Movshovitz-Attias, T. Kanade, and Y. Sheikh, "How useful is photo-realistic rendering for visual learning?," in *European Conference on Computer Vision*, 2016, pp. 202–217.
- [5] J. Tobin, R. Fong, A. Ray, J. Schneider, W. Zaremba, and P. Abbeel, "Domain Randomization for Transferring Deep Neural Networks from Simulation to the Real World," *IEEE Int. Conf. Intell. Robot. Syst.*, vol. 2017-Sept, pp. 23–30, 2017.
- [6] J. Tremblay, T. To, B. Sundaralingam, Y. Xiang, D. Fox, and S. Birchfield, "Deep Object Pose Estimation for Semantic Robotic Grasping of Household Objects," in *Conference on Robot Learning*, 2018.
- [7] J. Tremblay *et al.*, "Training deep networks with synthetic data: Bridging the reality gap by domain randomization," in *IEEE Conference on Computer Vision and Pattern Recognition Workshops*, 2018, pp. 1082–1090.
- [8] A. Prakash *et al.*, "Structured Domain Randomization: Bridging the Reality Gap by Context-Aware Synthetic Data," in *IEEE International Conference on Robotics and Automation*, 2019.
- [9] A. Rozantsev, V. Lepetit, and P. Fua, "On Rendering Synthetic Images for Training an Object Detector," *Comput. Vis. Image Underst.*, vol. 137, pp. 24–37, Aug. 2015.
- [10] S. R. Richter, V. Vineet, S. Roth, and V. Koltun, "Playing for Data: Ground Truth from Computer Games," in *European Conference on Computer Vision*, 2016.
- [11] A. Handa, V. Patraucean, V. Badrinarayanan, S. Stent, and R. Cipolla, "SceneNet: Understanding Real World Indoor Scenes With Synthetic Data," *arXiv Prepr. arXiv1511.07041v2*, Nov. 2015.
- [12] A. Gupta, A. Vedaldi, and A. Zisserman, "Synthetic Data for Text Localisation in Natural Images," *IEEE Conf. Comput. Vis. Pattern Recognit.*, Apr. 2016.
- [13] X. Peng, B. Sun, K. Ali, and K. Saenko, "Learning Deep Object Detectors from 3D Models," in *IEEE International Conference on Computer Vision*, 2015.
- [14] H. Su, C. R. Qi, Y. Li, and L. Guibas, "Render for CNN: Viewpoint Estimation in Images Using CNNs Trained with Rendered 3D Model Views," in *IEEE International Conference on Computer Vision*, 2015, pp. 2686–2694.
- [15] D. Dwibedi, I. Misra, and M. Hebert, "Cut, Paste and Learn: Surprisingly Easy Synthesis for Instance Detection," in *IEEE International Conference on Computer Vision*, 2017, pp. 1310–1319.
- [16] G. Georgakis, A. Mousavian, A. Berg, and J. Kosecka, "Synthesizing Training Data for Object Detection in Indoor Scenes," *arXiv Prepr. arXiv1702.07836v2*, 2017.
- [17] D. G. Lowe, "Distinctive Image Features from Scale-Invariant Keypoints," *Int. J. Comput. Vis.*, pp. 1–28, 2004.
- [18] H. Bay, A. Ess, T. Tuytelaars, and L. Van Gool, "Speeded-Up Robust Features (SURF)," *Comput. Vis. Image Underst.*, vol. 110, no. 3, pp. 346–359, 2008.
- [19] S. Hinterstoisser *et al.*, "Multimodal Templates for Real-Time Detection of Texture-less Objects in Heavily Cluttered Scenes," in *IEEE International Conference on Computer Vision*, 2011, pp. 858–865.
- [20] V. Ferrari, T. Tuytelaars, and L. Van Gool, "Object detection by contour segment networks," in *European Conference on Computer Vision*, 2006, pp. 14–28.
- [21] K. Simonyan and A. Zisserman, "Very Deep Convolutional Networks for Large-Scale Image Recognition," in *International Conference on Learning Representations*, 2014, pp. 1–14.
- [22] C. Szegedy *et al.*, "Going Deeper with Convolutions," in *IEEE Conference on Computer Vision and Pattern Recognition*, 2015, pp. 1–9.
- [23] K. He, X. Zhang, S. Ren, and J. Sun, "Deep Residual Learning for Image Recognition," in *IEEE Conference on Computer Vision and Pattern Recognition*, 2016, vol. 2016-Decem, pp. 770–778.
- [24] A. Krizhevsky, I. Sutskever, and G. E. Hinton, "ImageNet Classification with Deep Convolutional Neural Networks," in *Neural Information Processing Systems*, 2012, pp. 1097–1105.
- [25] J. Deng *et al.*, "ImageNet: A Large-Scale Hierarchical Image Database," in *IEEE Conference on Computer Vision and Pattern Recognition*, 2009.
- [26] B. Kulis, K. Saenko, and T. Darrell, "What You Saw is Not What You Get: Domain Adaptation Using Asymmetric Kernel Transforms," in *IEEE Conference on Computer Vision and Pattern Recognition*, 2011, pp. 1785–1792.
- [27] B. Gong, Y. Shi, F. Sha, and K. Grauman, "Geodesic Flow Kernel for Unsupervised Domain Adaptation," in *IEEE Conference on Computer Vision and Pattern Recognition*, 2012, pp. 2066–2073.
- [28] B. Fernando, A. Habrard, M. Sebban, and T. Tuytelaars, "Unsupervised Visual Domain Adaptation Using Subspace Alignment," in *IEEE International Conference on Computer Vision*, 2013.
- [29] B. Sun, J. Feng, and K. Saenko, "Return of Frustratingly Easy Domain Adaptation," in *AAAI Conference on Artificial Intelligence*, 2016, no. 1, pp. 2058–2065.
- [30] R. Gopalan, R. Li, and R. Chellappa, "Domain Adaptation for Object Recognition: An Unsupervised Approach," in *IEEE International Conference on Computer Vision*, 2011, pp. 999–1006.
- [31] L. Duan, I. W. Tsang, and D. Xu, "Domain Transfer Multiple Kernel Learning," *IEEE Trans. Pattern Anal. Mach. Intell.*, vol. 34, no. 3, pp. 465–479, 2012.
- [32] F. M. Carlucci, L. Porzi, B. Caputo, E. Ricci, and S. R. Bulò, "AutoDIAL: Automatic Domain Alignment Layers," in *IEEE International Conference on Computer Vision*, 2017, pp. 5077–5085.
- [33] M. Ghifary, W. B. Kleijn, M. Zhang, D. Balduzzi, and W. Li, "Deep Reconstruction-Classification Networks for Unsupervised Domain Adaptation," in *European Conference on Computer Vision*, 2016.
- [34] Y. Wang, W. Li, D. Dai, and L. Van Gool, "Deep Domain Adaptation by Geodesic Distance Minimization," in *IEEE International Conference on Computer Vision Workshops*, 2018, pp. 2651–2657.
- [35] Y. Ganin and V. Lempitsky, "Unsupervised Domain Adaptation by Backpropagation," in *International Conference on Machine Learning*, 2015, vol. 37.
- [36] O. Sener, H. O. Song, A. Saxena, and S. Savarese, "Learning Transferrable Representation for Unsupervised Domain Adaptation," in *Neural Information Processing Systems*, 2016.
- [37] P. Haeusser, T. Frerix, A. Mordvintsev, and D. Cremers, "Associative Domain Adaptation," *IEEE Int. Conf. Comput. Vis.*, pp. 2784–2792, 2017.
- [38] S. Motiian, M. Piccirilli, D. A. Adjeroh, and G. Doretto, "Unified Deep Supervised Domain Adaptation and Generalization," *Proc. IEEE Int. Conf. Comput. Vis.*, pp. 5716–5726, 2017.
- [39] J. Xu, S. Ramos, D. Vazquez, and A. M. Lopez, "Domain Adaptation of Deformable Part-Based Models," *IEEE Trans. Pattern Anal. Mach. Intell.*, vol. 36, no. 12, pp. 2367–2380, 2014.
- [40] B. Sun and K. Saenko, "From virtual to reality: Fast adaptation of virtual object detectors to real domains," in *British Machine Vision Conference*, 2014.
- [41] A. Raj, V. P. Namboodiri, and T. Tuytelaars, "Subspace Alignment Based Domain Adaptation for RCNN Detector," in *British Machine Vision Conference*, 2015.
- [42] Y. Chen, W. Li, C. Sakaridis, D. Dai, and L. Van Gool, "Domain Adaptive Faster R-CNN for Object Detection in the Wild," in *IEEE Computer Vision and Pattern Recognition*, 2018, pp. 3339–3348.
- [43] J. Hoffman *et al.*, "CyCADA: Cycle-Consistent Adversarial Domain adaptation," in *International Conference on Machine Learning*, 2018, vol. 5, pp. 3162–3174.
- [44] A. Dundar, M.-Y. Liu, T.-C. Wang, J. Zedlewski, and J. Kautz, "Domain Stylization: A Strong, Simple Baseline for Synthetic to

- Real Image Domain Adaptation,” *arXiv Prepr. arXiv1807.09384*, 2018.
- [45] J. Y. Zhu, T. Park, P. Isola, and A. A. Efros, “Unpaired Image-to-Image Translation Using Cycle-Consistent Adversarial Networks,” in *IEEE International Conference on Computer Vision*, 2017, pp. 2242–2251.
- [46] X. Huang, M. Y. Liu, S. Belongie, and J. Kautz, “Multimodal Unsupervised Image-to-Image Translation,” in *European Conference on Computer Vision*, 2018, pp. 179–196.
- [47] S. Ben-David, J. Blitzer, K. Crammer, A. Kulesza, F. Pereira, and J. W. Vaughan, “A theory of learning from different domains,” *Mach. Learn.*, vol. 79, pp. 151–175, 2010.
- [48] A. Singh, J. Sha, K. S. Narayan, T. Achim, and P. Abbeel, “BigBIRD: A Large-Scale 3D Database of Object Instances,” in *IEEE International Conference on Robotics and Automation*, 2014.
- [49] K. Lai, L. Bo, X. Ren, and D. Fox, “A large-scale hierarchical multi-view RGB-D object dataset,” in *IEEE International Conference on Robotics and Automation*, 2011, pp. 1817–1824.
- [50] C. Rother, V. Kolmogorov, and A. Blake, “‘GrabCut’ - Interactive Foreground Extraction using Iterated Graph Cuts,” in *SIGGRAPH*, 2004.
- [51] H. Noh, S. Hong, and B. Han, “Learning Deconvolution Network for Semantic Segmentation,” in *IEEE International Conference on Computer Vision*, 2015, vol. 1, pp. 1520–1528.
- [52] J. Long, E. Shelhamer, and T. Darrell, “Fully Convolutional Networks for Semantic Segmentation,” in *IEEE Conference on Computer Vision and Pattern Recognition*, 2015, pp. 3431–3440.
- [53] P. Ammirato, P. Poirson, E. Park, J. Kosecka, and A. C. Berg, “A Dataset for Developing and Benchmarking Active Vision,” in *Proceedings - IEEE International Conference on Robotics and Automation*, 2017, pp. 1378–1385.
- [54] G. Georgakis, M. A. Reza, A. Mousavian, P. H. Le, and J. Kosecka, “Multiview RGB-D dataset for object instance detection,” in *International Conference on 3D Vision*, 2016, pp. 426–434.
- [55] “SynDataGeneration.” [Online]. Available: <https://github.com/debidatta/syndata-generation>.
- [56] “faster-rcnn.pytorch.” [Online]. Available: <https://github.com/jwyang/faster-rcnn.pytorch>.
- [57] T. Y. Lin *et al.*, “Microsoft COCO: Common Objects in Context,” in *European Conference on Computer Vision*, 2014, pp. 740–755.
- [58] “MUNIT code.” [Online]. Available: <https://github.com/NVlabs/MUNIT>.
- [59] Y. Cho, J. Jeong, Y. Shin, and A. Kim, “DejavuGAN: Multi-temporal Image Translation toward Long-term Robot Autonomy,” in *IEEE International Conference on Robotics and Automation Workshops*, 2018.
- [60] S. Li, X. Xu, L. Nie, and T. S. Chua, “Laplacian-steered Neural Style Transfer,” in *ACM Multimedia*, 2017, pp. 1716–1724.
- [61] M. Everingham, S. M. A. Eslami, L. Van Gool, C. K. I. Williams, J. Winn, and A. Zisserman, “The Pascal Visual Object Classes Challenge: A Retrospective,” *Int. J. Comput. Vis.*, vol. 111, no. 1, pp. 98–136, 2014.
- [62] N. Silberman, D. Hoiem, P. Kohli, and R. Fergus, “Indoor Segmentation and Support Inference from RGBD Images,” in *European conference on Computer Vision*, 2012, vol. 5, pp. 746–760.
- [63] L. van der Maaten and G. Hinton, “Visualizing Data using t-SNE,” *J. Mach. Learn. Res.*, vol. 9, pp. 2579–2605, 2008.